



**Aligning Conservation Priorities Across Taxa in Madagascar with High-Resolution Planning Tools**  
C. Kremen, *et al.*  
*Science* **320**, 222 (2008);  
DOI: 10.1126/science.1155193

**The following resources related to this article are available online at [www.sciencemag.org](http://www.sciencemag.org) (this information is current as of April 14, 2008 ):**

**Updated information and services**, including high-resolution figures, can be found in the online version of this article at:

<http://www.sciencemag.org/cgi/content/full/320/5873/222>

**Supporting Online Material** can be found at:

<http://www.sciencemag.org/cgi/content/full/320/5873/222/DC1>

This article **cites 22 articles**, 2 of which can be accessed for free:

<http://www.sciencemag.org/cgi/content/full/320/5873/222#otherarticles>

This article appears in the following **subject collections**:

Ecology

<http://www.sciencemag.org/cgi/collection/ecology>

Information about obtaining **reprints** of this article or about obtaining **permission to reproduce this article** in whole or in part can be found at:

<http://www.sciencemag.org/about/permissions.dtl>

## References and Notes

- R. T. Shuey, *Semiconducting Ore Minerals*, vol. 4 of *Developments in Economic Geology* (Elsevier, Amsterdam, 1975).
- J. H. Kennedy, K. W. Frese, *J. Electrochem. Soc.* **125**, 723 (1978).
- C. Gleitzer, J. Nowotny, M. Rekas, *Appl. Phys. A Mat. Sci. Proc.* **53**, 310 (1991).
- B. A. Balko, K. M. Clarkson, *J. Electrochem. Soc.* **148**, E85 (2001).
- P. Venema, T. Hiemstra, P. G. Weidler, W. H. van Riemsdijk, *J. Colloid Interface Sci.* **198**, 282 (1998).
- F. Gaboriaud, J. Ehrhardt, *Geochim. Cosmochim. Acta* **67**, 967 (2003).
- C. G. B. Garrett, W. H. Brattain, *Phys. Rev.* **99**, 376 (1955).
- P. Mulvaney, V. Swayambunathan, F. Grieser, D. Meisel, *J. Phys. Chem.* **92**, 6732 (1988).
- R. M. Cornell, U. Schwertmann, *The Iron Oxides: Structure, Properties, Reactions, Occurrence and Uses* (VCH, Weinheim, Germany, 2003).
- T. Nakau, *J. Phys. Soc. Jpn.* **15**, 727 (1960).
- N. Iordanova, M. Dupuis, K. M. Rosso, *J. Chem. Phys.* **122**, 144305 (2005).
- J. S. LaKind, A. T. Stone, *Geochim. Cosmochim. Acta* **53**, 961 (1989).
- P. Mulvaney, R. Cooper, F. Grieser, D. Meisel, *Langmuir* **4**, 1206 (1988).
- A. G. B. Williams, M. M. Scherer, *Environ. Sci. Tech.* **38**, 4782 (2004).
- P. Larese-Casanova, M. M. Scherer, *Environ. Sci. Tech.* **41**, 471 (2007).
- D. Suter, C. Siffert, B. Sulzberger, W. Stumm, *Naturwissenschaften* **75**, 571 (1988).
- V. Barron, J. Torrent, *J. Colloid Interface Sci.* **177**, 407 (1996).
- C. M. Eggleston et al., *Geochim. Cosmochim. Acta* **67**, 985 (2003).
- T. P. Trainor et al., *Surf. Sci.* **573**, 204 (2004).
- O. W. Duckworth, S. T. Martin, *Geochim. Cosmochim. Acta* **65**, 4289 (2001).
- T. H. Yoon, S. B. Johnson, C. B. Musgrave, G. E. Brown, *Geochim. Cosmochim. Acta* **68**, 4505 (2004).
- J. R. Rustad, E. Wasserman, A. R. Felmy, *Surf. Sci.* **424**, 28 (1999).
- T. Hiemstra, W. H. Van Riemsdijk, *Langmuir* **15**, 8045 (1999).
- P. Zarzycki, *Appl. Surf. Sci.* **253**, 7604 (2007).
- Materials and methods are available on *Science Online*.
- M. J. Avena, O. R. Camara, C. P. Depauli, *Colloid Surf.* **69**, 217 (1993).
- N. Kallay, T. Preocanin, *J. Colloid Interface Sci.* **318**, 290 (2008).
- J. A. Davis, R. O. James, J. O. Leckie, *J. Colloid Interface Sci.* **63**, 480 (1978).
- B. Zinder, G. Furrer, W. Stumm, *Geochim. Cosmochim. Acta* **50**, 1861 (1986).
- S. Banwart, S. Davies, W. Stumm, *Colloid Surf.* **39**, 303 (1989).
- S. Kerisit, K. M. Rosso, *Geochim. Cosmochim. Acta* **70**, 1888 (2006).
- S. Kerisit, K. M. Rosso, *J. Chem. Phys.* **127**, 124706 (2007).
- N. M. Dimitrijevic, D. Savic, O. I. Micic, A. J. Nozik, *J. Phys. Chem.* **88**, 4278 (1984).
- J. P. Jolivet, E. Tronc, *J. Colloid Interface Sci.* **125**, 688 (1988).
- This research was supported by the U.S. Department of Energy (DOE), Office of Basic Energy Sciences, Geosciences Program. It was performed at the William R. Wiley Environmental Molecular Sciences Laboratory (EMSL) at the Pacific Northwest National Laboratory (PNNL). The EMSL is funded by the DOE Office of Biological and Environmental Research. PNNL is operated by Battelle for the DOE under contract DE-AC06-76RLO 1830. We gratefully acknowledge the assistance of C. Wang for TEM; B. Arey for scanning electron microscopy; D. McCready for pole reflection x-ray diffraction; Y. Lin for access to electrochemistry apparatus; and A. Felmy, E. Ilton, and J. Amonette for comments on an early version of this manuscript.

## Supporting Online Material

www.sciencemag.org/cgi/content/full/1154833/DC1  
Materials and Methods

Figs. S1 to S4  
References

4 January 2008; accepted 25 February 2008  
Published online 6 March 2008;  
10.1126/science.1154833  
Include this information when citing this paper.

# Aligning Conservation Priorities Across Taxa in Madagascar with High-Resolution Planning Tools

C. Kremen,<sup>1,2,\*†</sup> A. Cameron,<sup>1,2,†</sup> A. Moilanen,<sup>3</sup> S. J. Phillips,<sup>4</sup> C. D. Thomas,<sup>5</sup> H. Beentje,<sup>6</sup> J. Dransfield,<sup>6</sup> B. L. Fisher,<sup>7</sup> F. Glaw,<sup>8</sup> T. C. Good,<sup>9</sup> G. J. Harper,<sup>10</sup> R. J. Hijmans,<sup>11</sup> D. C. Lees,<sup>12</sup> E. Louis Jr.,<sup>13</sup> R. A. Nussbaum,<sup>14</sup> C. J. Raxworthy,<sup>15</sup> A. Razafimpahanana,<sup>2</sup> G. E. Schatz,<sup>16</sup> M. Vences,<sup>17</sup> D. R. Vieites,<sup>18</sup> P. C. Wright,<sup>19</sup> M. L. Zjhra<sup>9</sup>

Globally, priority areas for biodiversity are relatively well known, yet few detailed plans exist to direct conservation action within them, despite urgent need. Madagascar, like other globally recognized biodiversity hot spots, has complex spatial patterns of endemism that differ among taxonomic groups, creating challenges for the selection of within-country priorities. We show, in an analysis of wide taxonomic and geographic breadth and high spatial resolution, that multitaxonomic rather than single-taxon approaches are critical for identifying areas likely to promote the persistence of most species. Our conservation prioritization, facilitated by newly available techniques, identifies optimal expansion sites for the Madagascar government's current goal of tripling the land area under protection. Our findings further suggest that high-resolution multitaxonomic approaches to prioritization may be necessary to ensure protection for biodiversity in other global hot spots.

Approximately 50% of plant and 71 to 82% of vertebrate species are concentrated in biodiversity hot spots covering only 2.3% of Earth's land surface (1). These irreplaceable regions are thus among the highest global priorities for terrestrial conservation; reasonable consensus exists on their importance among various global prioritization schemes that identify areas of both high threat and unique biodiversity (2). The spatial patterns of species richness, endemism, and rarity of different taxonomic groups within priority areas, however, rarely align and are less well understood (3–6). Detailed

analysis of these patterns is required to allocate conservation resources most effectively (7, 8).

To date, only a few quantitative, high-resolution, systematic assessments of conservation priorities have been developed within these highly threatened and biodiverse regions (9, 10). This deficiency results from multiple obstacles, including limited data or access to data on species distributions and computational constraints on achieving high-resolution analyses over large geographic areas. We have been able to overcome each of these obstacles for Madagascar, a global conservation priority (1, 2, 11). Like many

other regions (3–6), Madagascar has complex, often nonconcordant patterns of microendemism among taxa (12–17), rendering the design of efficient protected-area networks particularly difficult (4, 6). We collated data for endemic species in six major taxonomic groups [ants, butterflies, frogs, geckos, lemurs, and plants (table S1)], using recent robust techniques in species distribution modeling (18, 19) and conservation planning (20, 21) to produce the first quantitative conservation prioritization for a biodiversity hot spot with this combination of taxonomic breadth (2315 species), geographic extent (587,040 km<sup>2</sup>), and spatial resolution (30-arc sec grid = ~0.86 km<sup>2</sup>).

Currently, an important opportunity exists to influence reserve network design in Madagascar, given the government's commitment, announced at the World Parks Congress in 2003, to triple its existing protected-area network to 10% coverage (22). Toward this goal, our high-resolution analysis prioritizes areas by their estimated contribution to the persistence of these 2315 species and identifies regions that optimally complement the existing reserve network in Madagascar.

We input expert-validated distribution models for 829 species and point occurrence data for the remaining species [those with too few occurrences to model, called rare target species (RTS)] into a prioritization algorithm, Zonation (20, 21), which generates a nested ranking of conservation priorities (23). Species that experienced a large proportional loss of suitable habitat (range reduction) between the years 1950 and 2000 were given higher weightings [equation 2 of (23), (24)]. We evaluated all solutions [defined here as the highest-ranked 10% of the landscape to match the target that Madagascar has set for conservation (22)] in two ways: (i) percent of species entirely

absent from the solution [“complete gaps” (11)] and (ii) proportional representation of species.

Avoiding complete gaps for all species considered, or “minimal representation,” is a basic goal of conservation prioritization (8) and can be accomplished in only 1020 grid squares (0.1% of the area of Madagascar) in a multitaxon analysis. The single-taxon solutions (fig. S1), however, did a poor job of minimally representing other species (Table 1) because of their low overlap (fig. S2). In single-taxon solutions, 25 to 50% of RTS species from other taxa were entirely omitted (Table 1A). Zero to 18% of modeled species were omitted, depending on whether evaluation was based on actual occurrence points (Table 1B) or distribution models (Table 1D). Overall, the use of any single-taxon solution would result in 16 to 39% of all species ending up as complete gaps (Table 1C, based on actual occurrence records).

In addition to ensuring minimal representation, our goal is to maximize proportional representation (the proportion of distribution or occurrence points) of species, especially those most vulnerable to extinction, in order to increase the probability of their persistence (11). In single-taxon solutions, we found that species from other taxa would often be represented at lower levels than the target taxon. Mean proportional representation for modeled species outside of the taxon was lower by a factor of 1.2 to 1.5 relative to the target taxon for all groups except plants (Fig. 1A), which include the most species and the smallest-ranged species within this data set,

making it comparatively difficult to protect large proportions of each species even in the plant-specific solution. Similarly, single-taxon solutions contained only 69 to 83%, on average, of the occurrence points for included (species that are represented by at least one record) RTS outside the target taxon, as compared to 100% of RTS records for species within the target taxon (Table 1E). Thus, any conservation prioritization based on a single surrogate taxon would be of limited utility for identifying conservation priorities across taxa in Madagascar.

The ideal solution to the surrogacy problem is to include all species in a single analysis (Fig. 2A), thus avoiding complete gaps (Table 1, last column) while optimizing proportional representation across all taxa. Until now, because of computational constraints, such analyses have not been feasible for this spatial resolution, geographic extent, and number of taxa. Figure S3A shows what can be achieved with the core-area Zonation method when used with weightings that account for historical range reductions. Without this weighting scheme, two species with the same current range size could be included at identical proportional representation, even though one had experienced a precipitous decline in range whereas the other had not. This approach thus prioritizes two classes of vulnerability. Narrow-ranged species, which are vulnerable to habitat loss coincident with their small ranges, are inherently prioritized by the Zonation algorithm [equation S1 of (23)]. Species that have suffered extensive recent range reductions (red dots in fig. S3) are additionally prioritized by their weightings, and the proportion of their historical (baseline) range included is thus increased.

Covering all six taxonomic groups simultaneously necessarily invokes tradeoffs, decreasing, for example, the proportions of species distributions represented in each taxon significantly relative to its own single-taxon solution (Fig. 1B,  $-0.04 \pm 0.002$  SE, paired Wilcoxon signed-ranks test,  $P < 0.0001$ ). To assess this tradeoff, we calculated a potential extinction risk for modeled species based on future distributional loss under the single- and multitaxon solutions, assuming loss of all habitat outside of prioritized areas and an aggregate species-area response (24). The increase in potential extinction risk for each taxonomic group incurred under the multitaxon solution relative to its own (fig. S4) constitutes the cost of including hundreds of species in the protected-area network that would otherwise be omitted (Table 1C).

We compared our multitaxon solution (Fig. 2A) against the actual parks selected during the recent protected-area expansion phase of 2002–2006 that has increased the total reserve coverage from 2.9 to 6.3% of Madagascar (Fig. 2B). The mean proportion of modeled species distributions included in the multitaxon solution (using the top 6.3% prioritized to compare with the area protected by 2006) was not significantly higher than in the actual selections ( $+0.004 \pm 0.002$  SE,

paired test, NS), as is expected because of tradeoffs among species (that is, given the fixed area of 6.3%, some species increased in representation when the optimized solution was compared to the actual solution, whereas others necessarily decreased, resulting in no mean change). The multitaxon solution, however, included all species, whereas the actual selections entirely omitted 28% of species (based on actual occurrence points, fig. S5). In addition, proportions included for the species with narrowest ranges or largest scores for the proportional range-reduction index were significantly larger in the multitaxon solution (at 6.3% of area) as compared to the actual selection [Kolmogorov-Smirnov two-sample test, first (smallest) quartile of range size,  $D = 0.28$ ,  $n = 207$  species,  $P < 0.001$ ; fourth (largest) quartile of proportional range-reduction index,  $D = 0.149$ ,  $n = 207$  species,  $P = 0.001$ ].

Finally, because we are operating in a real-world conservation context and many protected areas have already been established in Madagascar, we developed a realistic Zonation solution,

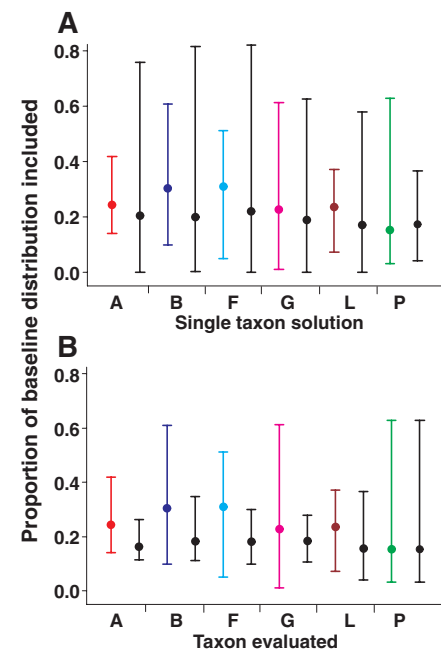


**Fig. 1.** Evaluating the top 10% of Zonation solutions for single- and multitaxon solutions. (A) The minimum, mean, and maximum proportion of the baseline (1950) distribution included for each taxonomic group [red, ants (A); blue, butterflies (B); cyan, frogs (F); pink, geckos (G); brown, lemurs (L); green, plants (P)] in its taxon-specific solution at 10% (fig. S1, A to F), compared to the corresponding mean and range for all other taxa (not including the solution taxon) if this particular single-taxon solution were to be adopted (black). (B) The minimum, mean, and maximum proportion of the baseline distribution included for each taxonomic group [colors and labels as in (A)] under its own individual solution (maps in fig. S1, A to F), compared to the values obtained for its taxonomic group only under the multitaxon solution (black, map in Fig. 2A).

<sup>1</sup>Department of Environmental Sciences, Policy and Management, 137 Mulford Hall, University of California, Berkeley, CA 94720-3114, USA. <sup>2</sup>Réseau de la Biodiversité de Madagascar, Wildlife Conservation Society, Villa Ifanomezantsoa, Soavimbahoaka, Boite Postale 8500, Antananarivo 101, Madagascar. <sup>3</sup>Metapopulation Research Group, Department of Biological and Environmental Sciences, Post Office Box 65, Viikinkaari 1, FI-00014, University of Helsinki, Finland. <sup>4</sup>AT&T Labs-Research, 180 Park Avenue, Florham Park, NJ 07932, USA. <sup>5</sup>Department of Biology (Area 18), University of York, Post Office Box 373, York YO10 5YW, UK. <sup>6</sup>Royal Botanic Gardens, Kew, Richmond TW9 3AB, Surrey, UK. <sup>7</sup>Department of Entomology, California Academy of Sciences, San Francisco, CA 94103, USA. <sup>8</sup>Zoologische Staatssammlung München, Münchhausenstrasse 21, 81247 München, Germany. <sup>9</sup>Department of Biology, Georgia Southern University, Statesboro, GA 30460, USA. <sup>10</sup>Conservation International, Center for Applied Biodiversity Science, 2011 Crystal Drive, Suite 500, Arlington, VA 22202, USA. <sup>11</sup>International Rice Research Institute, Los Baños, Philippines. <sup>12</sup>Department of Entomology, Natural History Museum, London SW7 5BD, UK. <sup>13</sup>Center for Conservation and Research, Henry Dooley Zoo, Omaha, NE 68107, USA. <sup>14</sup>Museum of Zoology, University of Michigan, Ann Arbor, MI 48109-1079, USA. <sup>15</sup>American Museum of Natural History, Central Park West at 79th Street, New York, NY 10024-5192, USA. <sup>16</sup>Missouri Botanical Garden, Post Office Box 299, St. Louis, MO 63166-0299, USA. <sup>17</sup>Zoological Institute, Technical University of Braunschweig, 38106 Braunschweig, Germany. <sup>18</sup>Museum of Vertebrate Zoology and Department of Integrative Biology, University of California, 3101 Valley Life Sciences Building, Berkeley, CA 94720-3160, USA. <sup>19</sup>Department of Anthropology, State University of New York, Stony Brook, NY 11794, USA.

\*To whom correspondence should be addressed. E-mail: ckremen@nature.berkeley.edu

†These authors contributed equally to this work.

optimized to expand on existing protected areas (6.3%) by adding an additional 3.7% of area (Fig. 2B, constrained solution). Like the unconstrained solution (Fig. 2A and Table 1), this solution (Fig. 2B) omits no species. The proposed expansion achieves relatively large increases in mean proportional representation ( $+0.05 \pm 0.001$  SE of modeled species' distributions and  $+58.8 \pm 1.1\%$  SE of RTS' occurrences). Most important, it realizes gains among the most vulnerable species, because of both the algorithm (20, 21) and the weighting system used. Among modeled species, those that have already lost much of their range (Fig. 3, A to C; red indicates the highest quartile of proportional range-reduction index) or are currently narrow-ranged (Fig. 3, D to F; red indicates the smallest quartile of range) increase most in proportional representation when moving from current parks (Fig. 3, B and E) to the con-

strained optimized solution (Fig. 3, C and F). For RTS species, expansion from current parks to the optimized solution would increase mean proportional representation to  $99.9 \pm 0.1\%$  SE of occurrences from 0% for gap species (39% of all RTS, fig. S5) or  $67.8 \pm 1.9\%$  SE for included species (fig. S6). Thus, although the protected areas selected to date have captured a relatively high proportion of Madagascar's species (~70% of species considered here, fig. S5), careful selection of the remaining 3.7% of area (as in the plan proposed in Fig. 2B) can produce further substantial conservation gains, both by including many more species and by increasing the proportional representation of the most vulnerable ones.

Our analysis provides fresh insights into conservation needs for Madagascar, identifying, for example, several regions within the central plateau massifs and littoral forests as priorities

(Fig. 2): areas with relatively low forest cover but considerable endemism that have been historically neglected in favor of protecting large forest blocks. Although our national-scale analysis identifies important biodiversity priorities at high resolution, precise delineation of protected areas requires taking socioeconomic factors into account (25). Within these priority areas, those that are most vulnerable to habitat destruction or are most highly ranked (fig. S7) should receive immediate attention (26). Although conservation areas must be identified by the end of 2008, final refinement and legal designation will not be completed until 2012. Thus, time is available for implementation of an iterative process (8): re-running this analysis to select optimal replacement sites each time areas within the solution are definitively rejected or destroyed, or alternate areas are definitively selected. Such updates could

**Table 1.** Surrogacy of higher taxa, comparing single- and multitaxon solutions. Section A, percentage of complete gap species for RTS species ( $n = 1486$ ). B, percentage of complete gap species for modeled species ( $n = 829$ ). C, percentage of complete gap species for all species (modeled and RTS,  $n = 2315$ ). Sections A, B, and C are based on occurrence data, and complete gaps are species with no points included in the solution. The diagonals and the

multitaxon columns have no unrepresented species, demonstrating as expected that Zonation includes all species considered within its solution. For D, the gap analysis was performed with models rather than occurrence points. E, mean percent of occurrence points included for nongap RTS species (species represented by at least one point in the solution). n.a., not applicable because all species are included in the solution by definition.

	Taxon assessed	Taxon targeted by zonation solution						
		Ants	Butterflies	Frogs	Geckos	Lemurs	Plants	All taxa
A. Percent of unmodeled (RTS) species unrepresented, based on point occurrence records	Ants	0	21.3	28.9	33.6	32.4	26.9	0
	Butterflies	14.5	0	22.1	25.2	38.9	24.4	0
	Frogs	34.1	25.7	0	30.7	25.7	21.2	0
	Geckos	26.9	23.1	23.1	0	26.9	19.2	0
	Lemurs	42.9	50.0	50.0	71.4	0	35.7	0
	Plants	45.2	52.3	42.8	62.2	54.8	0	0
	All species except target taxon	40.0	42.4	37.7	50.2	45.5	24.5	n.a.
B. Percent of modeled species unrepresented, based on point occurrence records	Ants	0	0	5.5	2.7	0	0	0
	Butterflies	0	0	4.7	0.6	0	0.6	0
	Frogs	5.0	5.0	0	5.0	0	0	0
	Geckos	0	0	0	0	0	0	0
	Lemurs	3.2	6.5	3.2	9.7	0	0	0
	Plants	13.3	14.1	23.4	26.2	16.4	0	0
	All species except target taxon	9.3	11.4	16.4	17.5	10.5	0.3	n.a.
C. Percent of modeled and RTS unrepresented, based on point occurrence records	All species except target taxon	28.3	32.3	29.6	38.5	33.2	16.2	0
D. Percent of modeled species with no part of their model protected by the Zonation solution	Ants	0	0	0	0	0	0	0
	Butterflies	0	0	1.2	0	0	0	0
	Frogs	0	0	0	0	0	0	0
	Geckos	0	0	0	0	0	0	0
	Lemurs	0	0	3.2	0	0	0	0
	Plants	1.6	0.4	8.0	2.0	1.6	0	0
	All species except target taxon	1.1	0.3	5.4	1.2	1.0	0.0	n.a.
E. Mean percent point occurrence records included for (nongap) RTS species only	Ants	100.0	84.9	87.6	80.5	75.7	77.1	100.0
	Butterflies	77.4	100.0	84.3	81.0	68.9	70.1	100.0
	Frogs	71.8	75.7	100.0	75.4	76.2	75.5	100.0
	Geckos	75.7	73.7	74.8	100.0	64.3	69.9	100.0
	Lemurs	68.1	49.9	45.6	39.0	100.0	56.3	100.0
	Plants	65.7	66.5	71.6	65.9	61.1	99.9	99.86
	All species except target taxon	68.7	72.8	76.6	72.7	67.5	74.4	n.a.

**Fig. 2.** Conservation priority zones in Madagascar. **(A)** Unconstrained multitaxon solution, showing what would have been selected based on these 2315 species if no areas were already protected. Colors indicate priority level: The top-ranked 2.9% priority areas are shaded yellow (equivalent to the area actually protected by 2002), the next-ranked priorities to 6.3% are blue (equivalent to the area actually protected by 2006), and the next-ranked priorities to 10% (equivalent to the conservation target) are red. **(B)** Constrained multitaxon solution, expanding (red) from existing parks in 2006 (yellow + blue = 6.3% of area) to 10% protection. The red areas are thus those that our analysis selects as the most important areas to consider for expansion of the current reserve network.

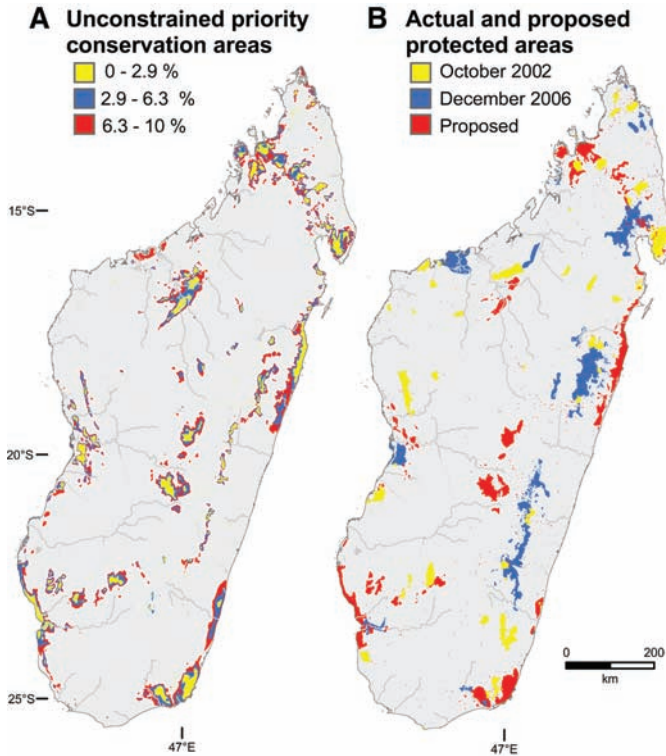
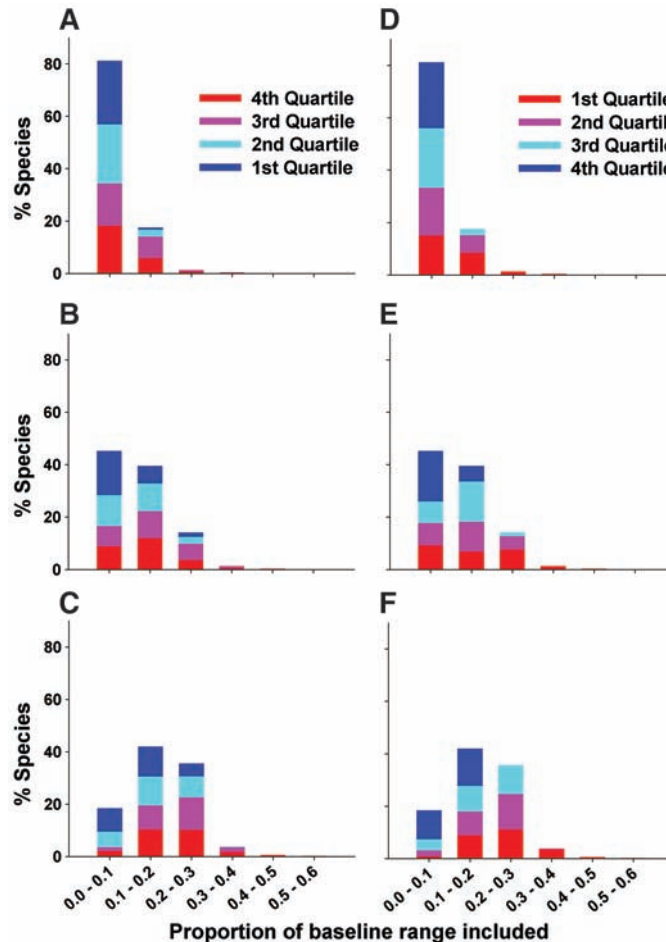


**Fig. 3.** Proportions of baseline (1950) species ranges (modeled) included at different phases of park expansion, as frequency histograms. **(A to C)** Within each histogram, species are coded by their proportional range-reduction index (weights used in Zonation), binned by quartiles, with the fourth quartile (red) representing the largest reductions. **(D to F)** Within each histogram, species are coded by their current range size, binned by quartiles, with the first quartile (red) representing the smallest-ranged species. **[(A) and (D)]** Protected areas designated by the year 2002, equaling 2.3% of the landscape (shaded yellow in Fig. 2B). **[(B) and (E)]** Protected areas designated by the year 2006, 6.3% of the landscape (shaded yellow and blue in Fig. 2B). **[(C) and (F)]** Constrained optimized expansion to 10% of the landscape (shaded yellow, blue, and red in Fig. 2B).



incorporate other taxonomic groups, new species records, and changing species designations (27). Our results suggest that conducting comparable analyses for other globally biodiverse areas is not only feasible but necessary, because of the inadequacy of single-taxon analyses to identify cross-taxon priorities and the need to develop high-resolution priorities within hot spots. As conservation targets are approached, optimization techniques become particularly critical to guide the final, toughest choices, so as to increase both the future representation of species in reserves and the probability that populations of these species will persist.

**References and Notes**

1. R. A. Mittermeier *et al.*, *Hotspots Revisited: Earth's Biologically Richest and Most Endangered Terrestrial Ecoregions* (Conservation International, Univ. of Chicago Press, Chicago, 2005).
2. T. M. Brooks *et al.*, *Science* **313**, 58 (2006).
3. R. Grenyer *et al.*, *Nature* **444**, 93 (2006).
4. A. S. van Jaarsveld *et al.*, *Science* **279**, 2106 (1998).
5. C. Moritz *et al.*, *Proc. R. Soc. London Ser. B* **268**, 1875 (2001).
6. J. R. Prendergast, R. M. Quinn, J. H. Lawton, B. C. Eversham, *Nature* **365**, 335 (1993).
7. R. M. Cowling, R. L. Pressey, A. T. Lombard, P. G. Desmet, A. G. Ellis, *Divers. Distrib.* **5**, 51 (1999).
8. C. R. Margules, R. L. Pressey, *Nature* **405**, 243 (2000).
9. R. M. Cowling, R. L. Pressey, M. Rouget, A. T. Lombard, *Biol. Conserv.* **112**, 191 (2003).
10. A. T. Knight *et al.*, *Conserv. Biol.* **20**, 739 (2006).
11. A. S. L. Rodrigues *et al.*, *Bioscience* **54**, 1092 (2004).
12. M. J. Raheerilalao, S. M. Goodman, *Rev. Ecol. Terre Vie* **60**, 355 (2005).
13. C. J. Raxworthy, R. A. Nussbaum, in *Biogeography of Madagascar*, W. R. Lourenco, Ed. (Orstom, Paris, 1996), pp. 369–383.
14. C. Kremen, D. C. Lees, J. Fay, in *Butterflies: Ecology and Evolution Taking Flight* (Univ. of Chicago Press, Chicago, 2003), pp. 517–540.
15. G. E. Schatz, C. Birkinshaw, P. P. Lowry II, F. Randriantafika, F. Ratovoson, in *Diversité et Endémisme à Madagascar*, W. C. Lourenco, S. M. Goodman, Eds. (Mémoires de la Société de Biogéographie, Paris, 2000), pp. 11–24.
16. G. E. Schatz, *Mem. Soc. Biogeogr. (Paris)* **2000**, 1 (2000).
17. S. Goodman, J. Benstead, *Oryx* **39**, 73 (2005).
18. J. Elith *et al.*, *Ecography* **29**, 129 (2006).
19. S. J. Phillips, R. P. Anderson, R. E. Schapire, *Ecol. Model.* **190**, 231 (2006).
20. A. Moilanen *et al.*, *Proc. R. Soc. London Ser. B* **272**, 1885 (2005).
21. A. Moilanen, *Biol. Conserv.* **134**, 571 (2007).
22. Gouvernement Malgache, *J. Off. Repub. Madagascar* **2004**, 2936 (2004).
23. Supporting material is available on Science Online.
24. C. D. Thomas *et al.*, *Nature* **427**, 145 (2004).
25. C. Kremen *et al.*, *Conserv. Biol.* **13**, 1055 (1999).
26. W. R. Turner, D. S. Wilcove, *Conserv. Biol.* **20**, 527 (2006).
27. J. Köhler *et al.*, *Bioscience* **55**, 693 (2005).
28. We thank C. Golden, C. Moritz, and W. Turner for valuable feedback on an earlier version. We are grateful to members of the Système d'Aires Protégées de Madagascar (SAPM) for facilitating the comparative work and for support from the MacArthur Foundation (grant no. 06-86791 to C.K.). The study was devised by C.K. and A.C. A.C. and C.K. conducted the analyses. A.M., S.J.P., and C.D.T. provided expert input on analytical methods and interpretation. R.J.H. and G.J.H. prepared environmental layers. A.C., H.B., J.D., B.L.F., F.G., T.C.G., C.K., D.C.L., E.L., R.A.N., C.J.R., G.E.S., M.V., D.R.V., P.C.W., and M.L.Z. contributed biodiversity data and

evaluated species distribution models and Zonation solutions for their taxa. A.R. conducted the geographic information system (GIS) analyses to produce the SAPM priority map (Fig. 2B, black outlines). C.K. and A.C. wrote the initial draft of the manuscript; all authors commented on subsequent drafts.

### Supporting Online Material

www.sciencemag.org/cgi/content/full/320/5873/222/DC1  
Methods  
SOM Text  
Figs. S1 to S11  
Table S1

### References

Extended Acknowledgments  
Appendix S1  
GIS data of Fig. 2  
14 January 2008; accepted 7 March 2008  
10.1126/science.1155193

# An Agonist of Toll-Like Receptor 5 Has Radioprotective Activity in Mouse and Primate Models

Lyudmila G. Burdelya,<sup>1\*</sup> Vadim I. Krivokrysenko,<sup>2\*</sup> Thomas C. Tallant,<sup>3</sup> Evguenia Strom,<sup>2</sup> Anatoly S. Gleiberman,<sup>2</sup> Damodar Gupta,<sup>1</sup> Oleg V. Kurnasov,<sup>4</sup> Farrel L. Fort,<sup>2</sup> Andrei L. Osterman,<sup>4</sup> Joseph A. DiDonato,<sup>3</sup> Elena Feinstein,<sup>2†</sup> Andrei V. Gudkov<sup>1,2†</sup>

The toxicity of ionizing radiation is associated with massive apoptosis in radiosensitive organs. Here, we investigate whether a drug that activates a signaling mechanism used by tumor cells to suppress apoptosis can protect healthy cells from the harmful effects of radiation. We studied CBLB502, a polypeptide drug derived from *Salmonella* flagellin that binds to Toll-like receptor 5 (TLR5) and activates nuclear factor- $\kappa$ B signaling. A single injection of CBLB502 before lethal total-body irradiation protected mice from both gastrointestinal and hematopoietic acute radiation syndromes and resulted in improved survival. CBLB502 injected after irradiation also enhanced survival, but at lower radiation doses. It is noteworthy that the drug did not decrease tumor radiosensitivity in mouse models. CBLB502 also showed radioprotective activity in lethally irradiated rhesus monkeys. Thus, TLR5 agonists could potentially improve the therapeutic index of cancer radiotherapy and serve as biological protectants in radiation emergencies.

The toxicity of high-dose ionizing radiation (IR) is associated with induction of acute radiation syndromes (1) involving the hematopoietic system (HP) and gastrointestinal tract (GI). The extreme sensitivity of HP and GI cells to genotoxic stress largely determines the adverse side effects of anticancer radiation therapy and chemotherapy (2). Development of radioprotectants for medical and biodefense applications has primarily focused on antioxidants that protect tissues (3) and cytokines that stimulate tissue regeneration (4).

Here, we have explored whether radioprotection can be achieved through suppression of apoptosis, the major mechanism underlying massive cell loss in radiosensitive tissues (5–7). Specifically, we have attempted to pharmacologically mimic an antiapoptotic mechanism frequently acquired by tumor cells, i.e., constitutive activation of the nuclear factor- $\kappa$ B (NF- $\kappa$ B) pathway (8). NF- $\kappa$ B is a transcription factor that plays a key role in cellular and organismal response to infectious agents as a mediator of innate and adaptive immune reactions. The link between NF- $\kappa$ B and the mammalian response to

IR has been established by previous work showing that GI radiosensitivity is enhanced in mice with a genetic defect in NF- $\kappa$ B signaling (9). Activation of NF- $\kappa$ B induces multiple factors that contribute to cell protection and promote tissue regeneration, including apoptosis inhibitors, reactive oxygen species scavengers, and cytokines. Finally, NF- $\kappa$ B activation is among the mechanisms by which tumors inhibit function of the p53 tumor suppressor pathway (10), one of the major determinants of radiosensitivity (11).

In order to activate NF- $\kappa$ B in GI cells without inducing acute inflammatory responses, we studied factors produced by benign microorganisms in the human gut that activate NF- $\kappa$ B by binding to Toll-like receptors (TLRs) expressed by host cells (12). Stimulation of TLR signaling by commensal microflora plays a protective role in the GI tract (13). In particular, we focused on TLR5, which is expressed on enterocytes, dendritic cells (14), and endothelial cells of the small intestine lamina propria (15). Endothelial cell apoptosis has been identified as an important contributor to the pathogenesis of GI acute radiation syndrome (16). The only known ligand and agonist of TLR5 is the bacterial protein flagellin (17).

To investigate whether flagellin has in vivo radioprotective activity, we injected flagellin purified from *Salmonella enterica* serovar Dublin (18) into NIH-Swiss mice 30 min before total-body  $\gamma$  irradiation (TBI). Treatment with 0.2 mg/kg of body weight of flagellin protected mice from lethal doses of 10 and 13 Gy that induce mortality

from HP and GI acute radiation syndromes, respectively (Fig. 1A). Flagellin did not rescue mice from 17 Gy TBI but prolonged their median survival from 7 to 12 days. The dose-modifying factor (DMF, the fold change in irradiation dose lethal for 50% of animals) of CBLB502 in NIH-Swiss mice was 1.6, exceeding that of other radioprotective compounds, such as cytokines or amifostine, used at nontoxic doses (3).

To reduce the immunogenicity and toxicity of flagellin, we took advantage of studies that mapped the TLR5-activating domains of flagellin to its evolutionarily conserved N and C termini (Fig. 1B) (19). We tested a series of engineered flagellin derivatives for NF- $\kappa$ B activation in vitro (Fig. 1B and fig. S1). The most potent NF- $\kappa$ B activator, designated CBLB502, included the complete N- and C-terminal domains of flagellin separated by a flexible linker (fig. S1). CBLB502 produced in *Escherichia coli* as a recombinant protein retains entirely the NF- $\kappa$ B-inducing activity and exceptional stability of flagellin (18), yet is substantially less immunogenic (fig. S2). It is also less toxic than flagellin, with a maximum tolerated dose (MTD) in mice of 25 mg/kg as compared with the 12 mg/kg MTD of flagellin (20). Flagellin derivatives that failed to activate NF- $\kappa$ B in vitro did not provide radioprotection in vivo (one example is shown in Fig. 1C), which suggested that activation of TLR5 signaling is necessary for radioprotection.

To test whether CBLB502 retained the radioprotective efficacy of flagellin, we administered a single injection of the compound (0.2 mg/kg) to NIH-Swiss mice 30 min before 13 Gy TBI. The treatment (18) rescued more than 87% of mice from radiation-induced death (Fig. 1C). At this radiation dose, the most powerful previously described radioprotectants provided about 54% protection [amifostine (21)] or had no protective effect at all [5-androstenediol (5-AED) or Neumune (22)] (Fig. 1C). Notably, the moderate protective effect observed with amifostine against 13 Gy TBI required injection of a dose (150 mg/kg) close to its MTD (200 mg/kg in NIH-Swiss mice). CBLB502 showed a significantly stronger protective effect ( $P < 0.05$ ) when it was injected at less than 1% of its MTD.

To address the practicality of CBLB502 as an antiradiation drug, we investigated the time frame for effective administration of the compound at different radiation doses. CBLB502 protected mice against the very high doses of radiation that induce lethal HP or combined HP and GI syndromes (10 Gy and 13 Gy, respectively) only when injected 15 to 60 min before TBI (Fig. 1D). The compound provided no survival benefit if injected before this time interval or after irradiation.

<sup>1</sup>Department of Cell Stress Biology, Roswell Park Cancer Institute, Buffalo, NY 14263, USA. <sup>2</sup>Cleveland BioLabs, Inc. (CBLI), Buffalo, NY 14203, USA. <sup>3</sup>Department of Cell Biology, Lerner Research Institute, Cleveland Clinic, Cleveland, OH 44195, USA. <sup>4</sup>Burnham Institute for Medical Research, La Jolla, CA 92037, USA.

\*These authors contributed equally to this work.

†To whom correspondence should be addressed. E-mail: andrei.gudkov@roswellpark.org; efeinstein@cblilabs.com

## **SUPPLEMENTARY ON-LINE MATERIALS**

### **Aligning conservation priorities across taxa in Madagascar with high-resolution planning tools**

C. Kremen, A. Cameron, A. Moilanen, S. Phillips, C. D. Thomas, H. Beentje, J. Dransfeld, B. L. Fisher, F. Glaw, T.C. Good, G. J. Harper, R. J. Hijmans<sup>0</sup>, D. C. Lees, E. Louis Jr., R. A. Nussbaum, C. J. Raxworthy, A. Razafimpahanana, G. E. Schatz, M. Vences, D. R. Vieites, P. C. Wright, M. L. Zjhra

## **METHODS**

### **MODELING OF SPECIES DISTRIBUTIONS**

#### ***Data***

All known species endemic to the Malagasy sub-region (*SI*) were included for the six major groups studied, unless noted otherwise in Table S1, which also lists the data sources and number of species within each of the six taxonomic groups. Point locality data (species occurrences) were standardised by each data provider in accordance with the most updated taxonomies available. After referencing point locality data to a 30 arc-second grid (0.86 km<sup>2</sup> at the Equator), all duplicates were eliminated from the database to reduce sample biases, unless they occurred in separate time periods (see Temporal Referencing, below). The Appendix provides species names, IUCN status, number of occurrence points after elimination of duplicates, and other information.

#### **Habitat Suitability Modeling**

We divided the species into two initial categories based on their number of available records (Table S1, Appendix). If the species had fewer than eight records, it was classified as a “Rare Target Species” (RTS) and we did not produce a habitat suitability model. Our division level of 8 records was based on several analyses examining the effect of sample size on model accuracy, which also showed that the

modeling technique used (Maxent) was particularly capable of producing good models with few records (S2) , and that one can model successfully with a small number of records given suitable model validation techniques (S3).

In comparative tests, the Maxent software(S4) (<http://www.cs.princeton.edu/~schapire/maxent>) that we used for this work has recently been found to be among the best modeling procedures for generating environmental niche predictions (S5). Maxent is a machine-learning technique which models a species' environmental niche as a probability distribution defined over the cells of the study area. The generated probability distribution is constrained to match the empirical averages of the environmental variables (and some functions thereof), determined using the species' point locality data. Among the probability distributions that satisfy all the constraints, the one of maximum entropy is chosen (S4). We refer to the Maxent output for a species as a habitat suitability map, with suitability values ranging continuously from 0 to 100. Since relatively few of our species had large numbers of distribution points, we further imposed stringent validation criteria in a two-part procedure to reject poor models (S2,S3).

## **Environmental Variables**

We used nine climate variables and a forest cover variable in modeling species distributions. Point locality data were spatially and temporally referenced against environmental layers (all on a 30 arc second grid) for climate ([www.worldclim.org](http://www.worldclim.org), S6) for two time periods (1930 to 1960 and 1950 to 2000), and for percent forest cover (S7) for four time periods (1950, 1970, 1990 and 2000). Mean monthly temperature, mean minimum monthly temperature, mean maximum monthly temperature, and average



monthly precipitation (mm) for the period 1950 to 2000 were downloaded from the WorldClim website (<http://worldclim.org>) (S6); we refer to these as our 2000, or current, climate layers for simplicity. We created matching climate layers for 1930-60 by downscaling data supplied by the Climate Research Unit; we refer to these as our 1950, or baseline, climate layers. The four climate layers were then used to generate the following sets of layers for the two time periods using ArcGIS 9.2 (ESRI).

1. RealMAT = Mean annual temperature (mean of monthly temperatures)
2. RealMAR = Mean annual precipitation (sum of mean monthly rainfall)
3. MinTemp = Mean temperature of the coldest month
4. MaxTemp = Mean temperature of the hottest month
5. MinPrec = Mean precipitation of the driest month
6. MaxPrec = Mean precipitation of the wettest month
7. ETPann = Annual total evapotranspiration.

First, monthly evapotranspiration rates ETP<sub>m</sub> (where m = values from 1 to 12 indicating calendar month) were calculated using the Thornthwaite equation (<http://leu.irnase.csic.es/microlei/manual2/cdbm/cdbm2e.html>):

$$ETP_m = 16 \times N_m \left( \frac{10 \times T_m}{I} \right)^a$$

Where  $T_m$  = mean temperature for month  $m$

$N_m$  = monthly adjustment factor relating to the number of hours of daylight

$$I = \text{Sum}(T_m/5)1.514$$

$$a = 6.75 \times 10^{-7} \times I^3 - 7.71 \times 10^{-5} \times I^2 + 1.792 \times 10^{-2} \times I + 0.49239$$

Annual total evapotranspiration (ETPann) was calculated by summing the 12 monthly evapotranspiration rates.

8. WBann = Annual water balance (mm)

$$WBann = \text{RealMAR} - \text{ETPann}$$

9. The number of months with a positive water balance (integer value between 1 and 12)

A map of forest cover change from the period 1950-2000 produced by Conservation International (CI) at 28.5 m resolution was utilized to develop forest cover layers for 1970, 1990 and 2000 (S7). This map was based on supervised classification of Landsat MSS, TM, and ETM images for the mid 1970s, circa 1990, and circa 2000, respectively, and utilized data from five days of aerial over-flights in 2002 for interpretation of satellite images and accuracy assessment. We separated this forest change map into individual forest cover layers for 1970, 1990, and 2000.

CI also provided a digitized version (S7) of the 1953 forest cover map produced by Humbert et al. in 1965 (S8), rasterized at the same resolution as the forest cover change map. The original map was produced from aerial photographs with ground-truthing. The 1953 study (S8) appears to have focused on mapping major forest blocks, as the map does not contain small fragments in remote areas that were present in later satellite images. We assumed that the additional small fragments present in 1970 had not grown in the intervening years, and hence any forest cover present in 1970 but absent in the 1953 map was added to the latter. To create a continuous variable matching the resolution of the climate layers, each of the four layers (1950, 1970, 1990, and 2000) at 28.5 m resolution was summarized as percent forest cover at a 30 arc-second grid cell size.

### **Temporal referencing of point data**

Because of the temporal spread in the point locality data (from 1802 to 2003) we used the “Samples With Data” format for inputting point locality data into Maxent,

ensuring that for each record, the environmental data was drawn from the era matching that record. Records from before 1975 were attributed climate data from the 1950 layers, and records from 1976 onwards were attributed climate data from the 2000 climate layers. Records from between 1950 and 1969, 1970 and 1989, 1990 and 1999, and after 2000 were attributed data from the 1950, 1970, 1990 and 2000 percent forest cover layers, respectively. If the record was from before 1949 it was attributed data from the 1950 forest cover layer, but if it occurred in a grid cell with less than 90% forest cover in 1950 it was excluded from the modeling data. Due to lack of information on forest cover conditions prior to 1950, attributing such a record to a cell which was not entirely forested in 1950 might lead to forest-dependent species being erroneously associated with non-forest or disturbed conditions in the models.

Duplicate species records for any individual grid cell were only retained if they were from different temporal periods (as defined above), meaning that they could contain different environmental data reflecting climate and/or habitat change in that location. If duplicate removal resulted in a species having fewer than 8 records it was dropped from the modeling group and assigned to the RTS species group.

## **Validation and error estimation of environmental niche models**

To reject poor predictions, first, all species with >8 independent points (grid squares) were modeled 100 times, randomly selecting 75% of the data for training and using the remaining 25% for testing. With the testing points, we calculated the Area under the Receiver Operating Characteristic Curves (AUC) for each of the 100 predictions per species. 1000 randomly generated background points were used in training the models, and a different randomized set of 1000 pseudo-absence points were

used for model-testing. Second, we accepted a species model only if the mean AUC value minus its 95% Confidence Interval was greater than 0.5. For species with less than 11 points, we used the actual number of training and testing combinations, which are  $< 100$ , to calculate the 95% Confidence Interval. Finally, for accepted species, we averaged all models per species to generate a mean habitat suitability surface.

### **Correcting for biogeographical over-prediction**

Habitat suitability models often over-predict species distributions because dispersal barriers and other biogeographic factors are not taken into account (S9). We created an algorithm to remove areas of over-prediction from the mean model in order to produce conservative models for conservation planning that closely represent areas of occupied habitat. This algorithm thresholds the model at a user defined habitat suitability value ( $t$ ), identifies regions above the threshold which contain observation points, draws a minimum convex hull around all such regions, and buffers the hull by a given number of grid cells ( $b$ ). Within the limits of this buffered hull the model values are retained, regardless of whether they are above  $t$ . Finally, a fading buffer width can also be set to a given number of grid cells ( $f$ ), within which the model values are linearly reduced until they reach zero.

We generated three versions to remove over-prediction using different thresholds and buffers:

Version 1:  $t = 40$ ,  $b = 40$ ,  $f = 80$

Version 2:  $t = 10$ ,  $b = 0$ ,  $f = 0$

Version 3:  $t = 40$ ,  $b = 0$ ,  $f = 0$

Figure S8a shows as an example the uncorrected mean model for the butterfly *Actizera atrigemmata* and its three biogeographically corrected models, along with its distribution points. Each data provider evaluated the three “corrected” versions against the original; across taxa, data providers for all taxonomic groups preferentially selected Version 1 (e.g. Fig S8b) as the best of the four models for the majority of their species. We subsequently used this version for all species in the conservation prioritizations. For each modeled species, its range size was defined in a threshold-independent manner as the sum of habitat suitability scores across the entire island.

## **CONSERVATION PRIORITY SETTING**

Madagascar’s President Marc Ravalomanana announced in 2003 at the World’s Park Congress in Durban, South Africa, the Government of Madagascar’s commitment to triple the protected areas network and thus to protect 10% of the land surface area (the “Durban Vision” target (S10)). At the time of the announcement, 1.7 million ha, or 2.9% of the 733,643 grid cells in the study, were already protected. Subsequently, during the period 2002-2006, an additional 2.18 million hectares have been awarded temporary protection status, increasing the landscape protected to 6.3%; these areas are now moving towards full protection. Mining and forestry activities have been suspended in a further 4 million hectares to accommodate conservation planning exercises that will identify the final 2.12 million hectares (3.74%), that will result in a total of 6 million hectares, or 10% of the landscape being protected.

## **Zonation algorithm**

The Zonation algorithm (S11, S12) differs philosophically from target-based planning or maximum coverage reserve selection (S13). Zonation does not operate to

meet hard targets assigned to species (or biodiversity features, in more generalized terms), but rather, a spatial conservation prioritization is generated based on trade-offs described between species. These trade-offs are defined by the weightings and connectivity responses assigned to species in the analysis. In addition, Zonation generates a hierarchy of nested solutions, instead of a single (near) optimal solution. The hierarchy is generated by the iterated removal of that cell whose loss causes the smallest decrease in the conservation value of the remaining reserve network, taking complementarity and connectivity into account. The final result is both a nested gradation of conservation priority throughout the landscape and an associated set of curves (see Fig S9 as an example) describing how well each species does at any given level of cell removal. We examined the top 10% ranked cells corresponding to 10% of the area of Madagascar, the conservation target under the government's pledge at the 2003 World Parks Congress.

The Zonation meta-algorithm is simple: (1) Start from the full landscape. Set rank  $r = 1$ . (2) Calculate marginal loss that would follow from the potential removal of each remaining grid cell  $i$ ,  $\delta_i$ . (3) Remove the cell with smallest  $\delta_i$ , set removal rank of  $i$  to be  $r$ , set  $r = r+1$ , and return to 2 if there are any cells remaining in the landscape. The critical part of the algorithm is the definition of marginal loss,  $\delta_i$ . To enhance for persistence of species in the landscape, we (1) used the Core-Area definition of marginal loss (see below), (2) used distribution smoothing to maintain higher connectivity (S11, S14), and (3) used weightings that accounted for past distribution loss since 1950 (see below).

Core-area Zonation gives highest value to locations with high habitat suitability levels for species. In particular, it does not treat habitat suitability scores as additive, meaning that ten cells with habitat suitability of 10 are seen as less valuable than a single location with a score of 100. At the start of any one iteration, Core-area Zonation defines marginal loss caused by the loss of cell  $i$  as:

$$\delta_i = \max_j \frac{q_{ij} w_j}{Q_j(S) c_i}, \quad (S1)$$

where  $w_j$  is the weight of species  $j$ ,  $c_i$  is the cost of adding cell  $i$  to the reserve network,  $q_{ij}$  is the local occurrence level of species  $j$  in cell  $i$ , and  $Q_j(S)$  is the fraction of the distribution of species  $j$  in the remaining set of grid cells,  $S$ . Equation (S1) thus integrates the cost of the cell, the priority (weight) given for the species, local occurrence levels and how much of its range each species has already been omitted during the course of the algorithm. It gives high rank to low-cost cells that have high occurrence levels for high-priority species. Heuristically, the lowest-priority cells, removed early in the Zonation process, are those that do not have high occurrence levels for any species of importance. The critical part of Equation (S1) is  $Q_j(S)$ , the proportion of the remaining range of species  $j$  located in cell  $i$  in the remaining set of cells,  $S$ . When a substantial part of the range of a species has been removed by the algorithm,  $Q_j(S)$  decreases, and the value of the remaining locations goes up. Thus, the last remaining localities for initially common species will have high value. Consequently, core-area Zonation retains important “core areas” of all species until the end of cell removal, even if the species is initially widespread and common. High-priority species that have narrow ranges will end up with relatively highest fractions of their ranges covered.

Compared to another variant for the cell removal rule, the additive benefit function rule, core-area Zonation produces lower mean but higher minimum representations across species, and the top ranking areas will have relatively higher local occurrence levels (habitat quality) for individual species. As a consequence, core-area Zonation will include high-quality core areas for each species even if the species richness in the area is low, whereas additive benefit function Zonation generally prioritizes areas of higher species-richness (S12). We preferred core-area Zonation because we wished to aim at balanced coverage of all species whether they occur in species-rich or species-poor areas.

The cell cost option (see Equation S1) was not utilized, i.e. cost was considered uniform across the landscape. In Madagascar, virtually all forested lands that are not yet protected are owned by the State (S15). Opportunity costs related to mining or forestry activities could differentiate cost among regions, but including opportunity cost was beyond the scope of this study. An area inclusion mask option was used for those runs that incorporated the existing protected areas. When using the mask, current protected areas (e.g. those areas designated by year 2006 totalling 6.3% of the country) were forcibly retained until all other cells had been removed from the landscape (S16). The outcome of our analyses utilizing the mask can be interpreted as answering the question, “What is the optimum expansion strategy from the currently protected areas of Madagascar according to the core-area Zonation rule?”.

The Zonation software and a user manual are freely available from <http://www.helsinki.fi/bioscience/consplan>. The only feature of Zonation used here that is not available in version 1.0 is allowing entry of species data both as continuous



surfaces (models) and point distributions. This possibility will be made available in a forthcoming update, v2.

## Weightings

We calculated an index of proportional range reduction, also known as the “fractional extinction risk” (cf. *S17*), to use as a weighting ( $w_j$ ) within Zonation for each species,  $j$ , based on the change in range size (defined in the threshold-independent manner described in the modeling section, above) between 1950 and 2000, and using the following equation:

$$w_j = 1 - (r_{j,2000} / r_{j,1950})^z \quad (S2)$$

where  $r_{j,2000}$  = the range size of species  $j$  in year 2000,  $r_{j,1950}$  = the range size of species  $j$  in 1950, and  $z=0.25$  (*S18*). These weightings are based on proportional range reduction and serve as relative measures of vulnerability in the absence of other species-specific information, such as information on population size, changes in population status, exploitation, etc. Species that experienced an increase in  $r_j$  from 1950 to 2000 ( $n=59$ ) were given  $w_j=0$ . We verified that such species were well-represented in the multi-taxon solution (Fig 2b) despite their low weightings (mean  $\pm$  S.E. of occurrences included =  $70\% \pm 3\%$  compared with  $73.6 \pm 0.6\%$  over all species; mean proportion of baseline range included  $\pm$  S.E =  $0.22 \pm 0.01$  compared with  $0.18 \pm 0.003$  over all species).

To assess further the relationship between these weightings and extinction risk, we ranked all species by their weightings (listed in Appendix) and assessed differences among taxonomic groups. Ninety-three percent of the species in the top quartile of

weightings were plants ( $X^2 = 115.73$ ,  $p < 0.001$ ). This accords well with several independent studies of plant vulnerability in Madagascar (*S19- S23*), suggesting exceptionally high risk of extinctions for a variety of plant groups in Madagascar.

## **Smoothing**

Smoothing corresponds to a metapopulation-dynamical connectivity calculation which effectively reduces the value of small, isolated fragments and increases the value of areas with a high density of suitable habitat (*S11, S24*). The smoothing process modifies each species habitat suitability model to produce a species-specific connectivity surface. The smoothing parameter is set using a parameter, alpha, which describes the dispersal ability or scale of landscape use of focal species. We used an alpha corresponding to a mean distance of 2 km using a negative exponential dispersal kernel (*S16*). While the scale of landscape use is unknown for most species in this dataset, 2 km is a reasonable approximation for landscape use by the largest species in our data set (the lemurs, *S25*). Effectively, this setting for smoothing indicates a belief that habitat loss within a few kilometres of the focal location may negatively influence meta-population dynamics and probability of population persistence for our set of species.

Smoothing has the benefit of producing a more aggregated reserve network (Fig *S10*), which is both more likely to maintain populations due to a lower level of fragmentation (*S14*) and is more realistic to implement on the ground. For each single taxon and the multi-taxon analysis, we created Zonation solutions with and without distribution smoothing, and then asked data providers to evaluate the results for their taxon and the multi-taxon solution. Data providers uniformly preferred the smoothed Zonation solutions; thus we only report results based on distribution smoothing.

## **Multi-taxon run**

It proved computationally impossible to conduct Zonation runs with all 2315 species at the resolution that we had selected for this analysis (30 arc sec grid with 733,643 grid cells). Rather than lose resolution, we instead reduced the area to be considered by excising areas identified as low priority across all of the single taxon solutions (Fig S11). To accomplish this, we first selected the top 25% of each single taxon solution, and then overlaid these layers. We identified all grid cells that never occurred in any of the top 25% regions for any taxon under any run conditions (i.e., for each single-taxon analysis, we separately examined the impact of smoothing or no smoothing, and of including RTS or not, unpublished analyses), and that also did not fall within an existing protected area. This region, occupying 27% of the country, consisted of heavily impacted agricultural and urban areas with low occurrence levels for species of conservation priority (Fig S11). Across all species, the median proportion of species ranges included in this region was 3.6% and the average 5.6%. This region was therefore excised (allocated no-data values) from all species distribution models prior to conducting the multi-taxon Zonation run.

## **Comparing and evaluating Zonation solutions**

We used geographic information system queries to conduct gap analyses based on occurrence data or modeled distributions, and to evaluate proportional representation for modeled species (based on distributions) or RTS (based on occurrence data). For modeled species, proportions of species ranges included were calculated against species' 1950s distributions as the best approximation of a historical baseline; results were qualitatively similar when calculated against current distributions in 2000. To assess the cost of including species outside of the target taxon, we calculated the potential extinction

risk (*S17*) for each taxonomic group within its single taxon solution and in the multi-taxon solution (Eqn 3, below).

### **Potential extinction risk calculations**

The calculation of potential extinction risk (*S17*) was based on the change in range size (summed habitat suitability) between the baseline year of 1950 and our future conservation scenario which assumes that only the protected regions identified by our solution will remain forested.

$$ER_{T, ZS} = \frac{1}{n} \sum_{j=1}^n \left( \frac{r_{j, ZS}}{r_{j, 1950}} \right)^z \quad (S3)$$

Potential extinction risk,  $ER_{T, ZS}$ , is the mean fractional extinction risk for a given taxon  $T$  in a given Zonation solution,  $ZS$ ;  $r_{j, ZS}$  = the range size of species  $j$  in the areas delineated by that Zonation solution;  $r_{j, 1950}$  = the range size of species  $j$  in 1950;  $n$  = number of species in  $T$ ; and  $z = 0.25$  for the species-area relationships (*S18*). This method of calculating extinction risk may overestimate risk because of the assumption that species will only persist inside protected areas, and not in the human-dominated landscape surrounding them (*S26*). To handle this in the analysis, we assigned those species whose ranges appeared to be expanding during the time period 1950-2000 (i.e. are responding favourably to human disturbance) a weighting of zero in Zonation runs (see above). In general, however, this index of extinction potential is more likely to underestimate extinction risk for at least three reasons. First, it does not include risk factors other than habitat destruction, such as exploitation, invasive species, or future climate change. Second, because we consider only species endemic to the Madagascar sub-region, and habitat loss for Madagascar exceeds 50%, species-area equations converge on endemic-

area relationships (S27, S28). In other words, extinction debt is not overestimated. Third, we do not account for area and distributional losses prior to 1950 (S7).

## References

- S1. S. Goodman, J. Benstead, *Oryx* **39**, 73 (2005).
- S2. P. A. Hernandez, C. H. Graham, L. L. Master, D. L. Albert, *Ecography* **29**, 773 (2006).
- S3. R. G. Pearson, C. J. Raxworthy, M. Nakamura, A. T. Peterson, *Journal of Biogeography* **34**, 102 (Jan, 2007).
- S4. S. J. Phillips, R. P. Anderson, R. E. Schapire, *Ecological Modeling* **190**, 231 (Jan, 2006).
- S5. J. Elith *et al.*, *Ecography* **29**, 129 (Apr, 2006).
- S6. R. J. Hijmans, S. E. Cameron, J. L. Parra, P. G. Jones, A. Jarvis, *International Journal of Climatology* **25**, 1965 (Dec, 2005).
- S7. G. Harper, M. Steininger, C. Tucker, D. Juhn, F. Hawkins, *Environmental Conservation*, In Press (2008).
- S8. H. Humbert, in *Notice de la carte de Madagascar. Travaux de la Section Scientifique et Technique de l'Institut Français de Pondichèrey, hors série H*. Humbert, G. C. Darne, Eds. (1965), vol. 6, pp. 46-78.
- S9. C. J. Raxworthy *et al.*, *Nature* **426**, 837 (Dec 18, 2003).
- S10. Gouvernement Malgache, in *Journal Officiel de la Republique de Madagascar*. (2004) pp. 2936.
- S11. A. Moilanen *et al.*, *Proceedings of the Royal Society B-Biological Sciences* **272**, 1885 (Sep, 2005).
- S12. A. Moilanen, *Biological Conservation* **134**, 571 (Feb, 2007).
- S13. C. R. Margules, R. L. Pressey, *Nature* **405**, 243 (May 11, 2000).
- S14. A. Moilanen, B. A. Wintle, *Biological Conservation* **129**, 427 (May, 2006).
- S15. C. Kremen *et al.*, *Conservation Biology* **13**, 1055 (1999).
- S16. A. Moilanen, H. Kujala. (Helsinki, Finland, 2006, <http://www.helsinki.fi/bioscience/consplan>) pp. 126 pp.
- S17. C. D. Thomas *et al.*, *Nature* **427**, 145 (Jan 8, 2004).
- S18. O. E. Sala, H. M. Van Vuuren, D. Pereira, L. D., in *Ecosystem and human well-being: scenarios*. (Island Press, Washington, DC, 2005) pp. 375-408.
- S19. T. C. Good, M. L. Zjhra, C. Kremen, *Conservation Biology* **20**, 1099 (Aug, 2006).
- S20. M. W. Callmander, G. E. Schatz, T. Consiglio, I. Lowry, Porter P., *Oryx* **41**, 168 (2007).
- S21. G. E. Schatz, P. P. Lowry II, A. E. Wolf, *Adansonia, ser. 3* **20**, 233 (1998).
- S22. G. E. Schatz, P. P. Lowry II, A. E. Wolf, *Adansonia*, 255 (1999).
- S23. G. E. Schatz, P. P. Lowry II, A. E. Wolf, *Adansonia*, 107 (1999).
- S24. A. Moilanen, B. A. Wintle, *Conservation Biology* **21**, 355 (Apr, 2007).
- S25. D. J. Overdorff, in *Lemur Social Systems and Their Ecological Basis* P. M. Kappeler, J. U. Ganzhorn, Eds. (Plenum Press, New York, 1993) pp. 167-178.
- S26. H. M. Pereira, G. C. Daily, *Ecology* **87**, 1877 (Aug, 2006).

- S27. J. R. Malcolm, C. R. Liu, R. P. Neilson, L. Hansen, L. Hannah, *Conservation Biology* **20**, 538 (Apr, 2006).
- S28. A. P. Kinzig, J. Harte, *Ecology* **81**, 3305 (Dec, 2000).
- S29. M. J. Raherilalao, S. M. Goodman, *Revue D Ecologie-La Terre Et La Vie* **60**, 355 (2005).
- S30. C. J. Raxworthy, R. A. Nussbaum, in *Biogeography of Madagascar* W. R. Lourenco, Ed. (Orstom, Paris, 1996) pp. 369-383.
- S31. C. Kremen, D. C. Lees, J. Fay, in *Butterflies: Ecology and Evolution Taking Flight*. (University of Chicago Press, Chicago, 2003) pp. 517-540.
- S32. G. E. Schatz, C. Birkinshaw, P. P. Lowry II, F. Randriantafika, F. Ratovoson, in *Diversité et Endémisme à Madagascar* W. C. Lourenco, S. M. Goodman, Eds. (Mémoires de la Société de Biogéographie, Paris, 2000) pp. 11-24.
- S33. G. E. Schatz, *Memoires de la Societe de Biogeographie (Paris)*, 1 (2000).
- S34. A. G. Bruner, R. E. Gullison, R. E. Rice, G. A. B. da Fonseca, *Science* **291**, 125 (2001).
- S35. J. Dufils, in *The Natural History of Madagascar* S. Goodman, J. P. Benstead, Eds. (University of Chicago Press, Chicago, 2003) pp. 88-96.
- S36. S. H. M. Butchart *et al.*, *Plos Biology* **2**, 2294 (2004).
- S37. D. C. Lees, C. Kremen, H. Raharitsimba, in *The Natural History of Madagascar*. (University Press Chicago, Chicago, 2003) pp. 762-791.
- S38. D. C. Lees, C. Kremen, L. Andriamampianina, *Biological Journal of the Linnean Society* **67**, 529 (1999).
- S39. C. Kremen, *Ecological Applications* **4**, 407 (1994).
- S40. C. Kremen, D. Lees, V. Razafimahatratra, H. Raharitsimba, in *African rain forest ecology and conservation* W. Weber, A. Vedder, H. S. Morland, L. White, T. Hart, Eds. (Yale University Press, New Haven, Connecticut, 2001) pp. 400-428.
- S41. A. Cameron, PhD, University of Leeds (2005).
- S42. C. Kremen, *Ecological Applications* **2**, 203 (1992).
- S43. F. Glaw, M. Vences, *Field guide to the amphibians and reptiles of Madagascar, Third edition* (Vences and Glaw-Verlag, Köln, Germany, 2007), pp.
- S44. L. Wilme, S. M. Goodman, J. U. Ganzhorn, *Science* **312**, 1063 (May, 2006).
- S45. Groupes d'Etudes de Recherches sur les Primates de Madagascar, "Annual report to the Makira Project" (2005).
- S46. P. Wright *et al.*, *Primate Conservation*. **23** (2008).
- S47. M. T. Irwin, S. E. Johnson, P. C. Wright, *Oryx* **39**, 204 (April, 2005).
- S48. M. A. Banks, E. R. Ellis, A. Wright, P. C. Wright, *Animal Conservation* **10**, 254 (May, 2007).
- S49. S. M. Lehman, M. Mayor, P. C. Wright, *American Journal of Physical Anthropology* **126**, 318 (March, 2005).
- S50. S. J. Arrigo-Nelson, P. C. Wright, *Folia Primatologica* **75**, 331 (2004).
- S51. R. A. Mittermeier *et al.*, in *Conservation International Tropical Field Guide Series*. (Washington D.C., 2006).
- S52. M. L. Zjhra, *Annales Botanici Fennici* **43**, 225 (Jun, 2006).
- S53. J. Dransfield, H. Beentje, *The palms of Madagascar* (Royal Botanic Gardens, Kew and The International Palm Society, London, UK, 1995), pp. 475.

**S54. Acknowledgements.**

Joseph Chipperfield assisted by writing scripts in Perl and C for data manipulation.

Butterflies: Heritiana Raharitsimba, Ranaivosolo Ravomiarana and Maminarina Ravoninjatovo assisted with collection of the butterfly data.

Frogs: Franco Andreone, Parfait Bora, Ignacio de la Riva, Euan Edwards, Jörn Köhler, Fabio Mattioli, Falitiana Rabemananjara, Liliane Raharivololoniaina, Daniel Rakotondravony, Roger Daniel Randrianiaina, Jasmin Randrianirina, Olga Ramilijaona, Noromalala Raminosoa, and Denis Vallan provided assistance during field surveys of frogs.

Geckos: S. Mahaviasy, N. Rabibisoa, D. Rakotondravony, A. Rakotondrazafy, J.B. Ramanamanjato, M. Randriambahiniarime, A. Ranjanaharisoa, A.P. Raselimanana, A. Razafimanantsoa, and A. Razafimanantsoa assisted with collection of the gecko data. Richard Pearson assisted with the preparation of gecko data, examination of model outputs and overall advice on species distribution modeling.

Lemurs: Felix Ratelolahy, Mitch Irwin, Steig Johnson, Chia Tan, Summer Arrigo-Nelson, Justin Solo, Jonah Ratsimbazafy, Shawn Lehman, Mireya Mayor, Toni Lyn Morelli, Jean Luc Raharison, Volontiana Razafindratsita and Matthew Banks assisted with lemur surveys. Christopher Golden assisted with validation of lemur species models.

Plants: Sylvie Andriambololonera, M. W. Callamander, Jeannie Raharimampionona, and Tantely Raminosoa assisted with preparation of the APAPC botanical data set. Specimens of Coleeae (Bignoniaceae), including types, were generously loaned by the Muséum National d'Histoire Naturelle, Paris, the Royal Botanic Gardens, Kew, and the Missouri Botanical Garden, St. Louis.

Systèmes d'Aires Protégées de Madagascar: The assistance of the members of the SAPM group are gratefully acknowledge, including Laurette Rasoavahiny, Directeur du Systèmes d'Aires Protégées (Ministère de l'Environnement, des Eaux et Forêt et du Tourisme), Nanie Ratsifandrihamanana (WWF), Herizo Andrianandrasana (Durell), Tantely Raminosoa (MBG), Rado Andriamasimanana (BIMP), Anjara Andriamanalina (WWF), Tiana Andriamanga (ANGAP), Mino Razafindramanga (ESSA-Forêt), Lucciano Andriamaro (CI), Harison Randrianasolo (CI), Michele Andrianarisata (CI), Tiana Ramahaleo (WWF), Balisama Rajemison (CAS), Aristide Andrianarimisa (WCS), Andry Rakotomanjaka (REBIOMA).

Funding: For published work, funding sources for field surveys were acknowledged in the primary publications resulting from the field work in question. Additional funding sources include Critical Ecosystem Partnership Fund (GES); National Science Foundation (DEB-0344731 to B.L.F. and P.S. Ward), Rufford Small Grants Foundation (AC), Leverhulme Trust (F/00696/I to DL), Norman and Lucile Packard Foundation (PCW), Margo Marsh Biodiversity Fund (PCW), Primate Conservation, Inc. (PCW), PrimateAction Fund (PCW), National Science Foundation (PCW), Deutsche

Kremen et al., *Aligning conservation priorities across taxa, SOM*

Forschungsgemeinschaft (MV, FG), Volkswagen Foundation (MV, FG), and NSF (Tree of Life grant EF, 1-10135 for DV), National Science Foundation to R.A.N and C.J.R (DEB 05-08584, DEB 04-23286, DEB 99-84496, DEB 96-25873, DEB93-22600, and BSR 90-24505), the National Geographic Society (5396-94 to CJR), Earthwatch (CJR), Worldwide Fund for Nature (CJR), and Conservation International (CJR).



## Figures

**Figure S1.** Conservation priority zones in Madagascar, showing the top 10% prioritized area in red for each of six single taxon solutions. Each taxon prioritizes principally different zones, reflecting differences in patterns of micro-endemism, species richness, and the ecological requirements of each group (S1, S29- S33). For example, priority areas for frogs (C) are restricted to the wetter eastern half of the island, whereas the other groups also show priority areas in the very dry south-western parts of Madagascar.

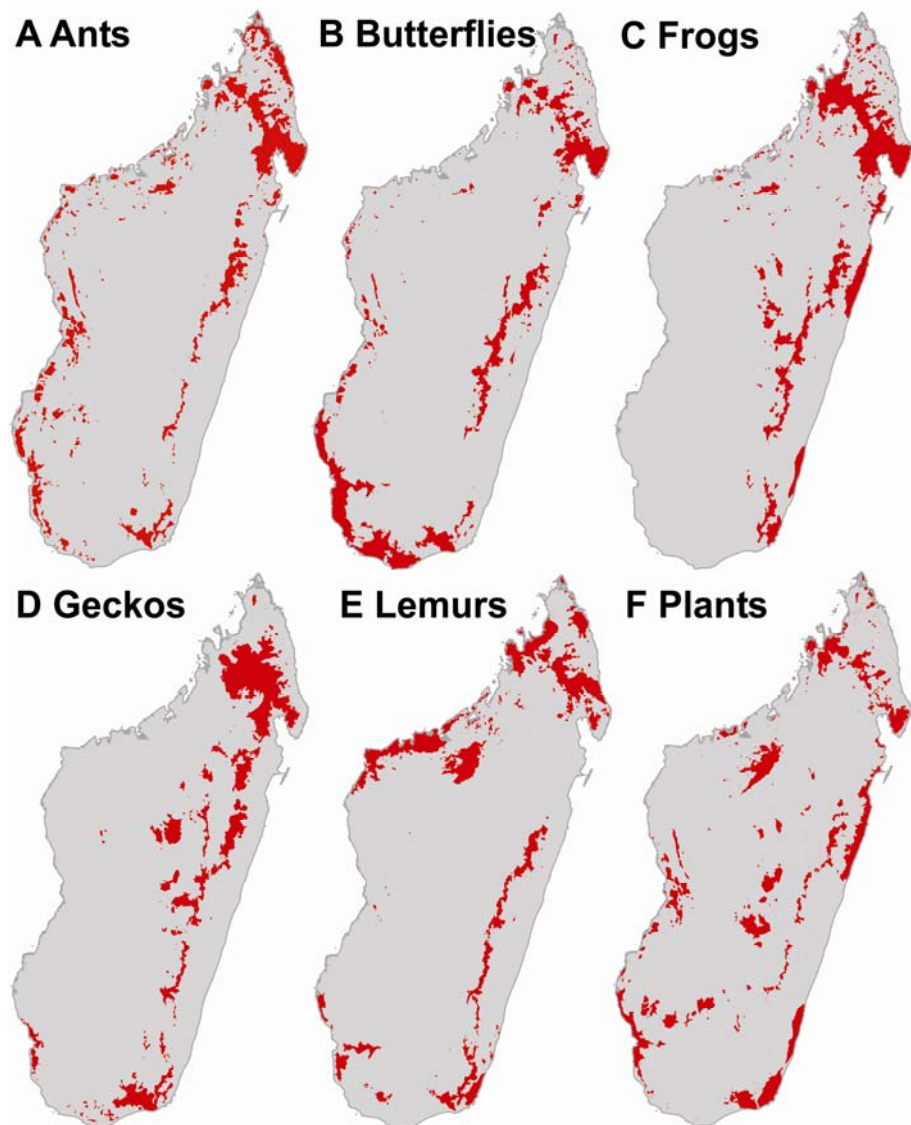


**Figure S2. Agreements and disagreements between the six single taxon solutions.** Combining the top 10% solutions for each of the six taxonomic groups (Fig. S1 A-F) results in an area of 26.4% of the country, shown here, which far exceeds the conservation target. This is due to low overlap between solutions: only 1.6% of the landscape was selected in common by all six single-taxon solutions, whereas 11.4% was unique to one of the single taxon solutions. Dark red shows agreement between all six single taxon solutions (Fig S1 a-f). Dark blue indicates areas important for only one taxon. Intermediate colours show 2-6 single-taxa in agreement.

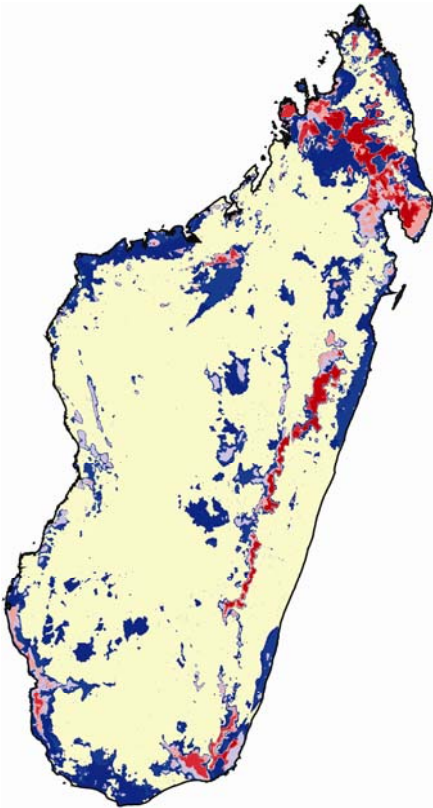


### Figure S3. Proportional representation of species achieved by core-area Zonation in the multi-taxon, unconstrained run.

a. The proportion of the baseline ranges (summed habitat suitability in 1950) of modeled species included, shown against baseline range size (summed habitat suitability in 1950).  
 b. The proportion of the current range (summed habitat suitability in 2000) of modeled species included, shown against current range size (summed habitat suitability in 2000).  
 In both panels, the dots for each species are colour-coded by an index of proportional range reduction resulting from habitat loss since 1950 (e.g. species weightings used in Zonation runs), which can be thought of as an important extinction risk factor (S36). Red = top (most threatened) quartile of proportional range reduction weightings, pink = 2nd quartile, grey = 3rd quartile, black = 4th quartile (least threatened). In panel a., it can be observed that most species which had large ranges in 1950 accumulated high extinction risk (red dots), due to losses of large portions of their original ranges in the intervening period. In contrast, species with small range sizes (micro-endemics) varied in proportional range reduction scores (all colours), although more had low risks (black and grey). By comparing panel a. and b., one can see that use of the proportional range reduction weighting ensures relatively high proportions of the species with greatest extinction risk (red dots) are included in the Zonation solution. Visually, as range sizes were reduced due to deforestation, red dots shift left from panel a. to b., due to range loss, and upwards, due to increased proportional representation, from baseline to current distributions. In panel b, it can also be seen that the highest proportions of current ranges included in the solution belong to the most range-restricted and thus most irreplaceable species. Some of these species were range-restricted (micro-endemics) in 1950 and have had little change in their ranges (grey and black dots) while others are newly range-restricted due to habitat loss (red and pink dots).

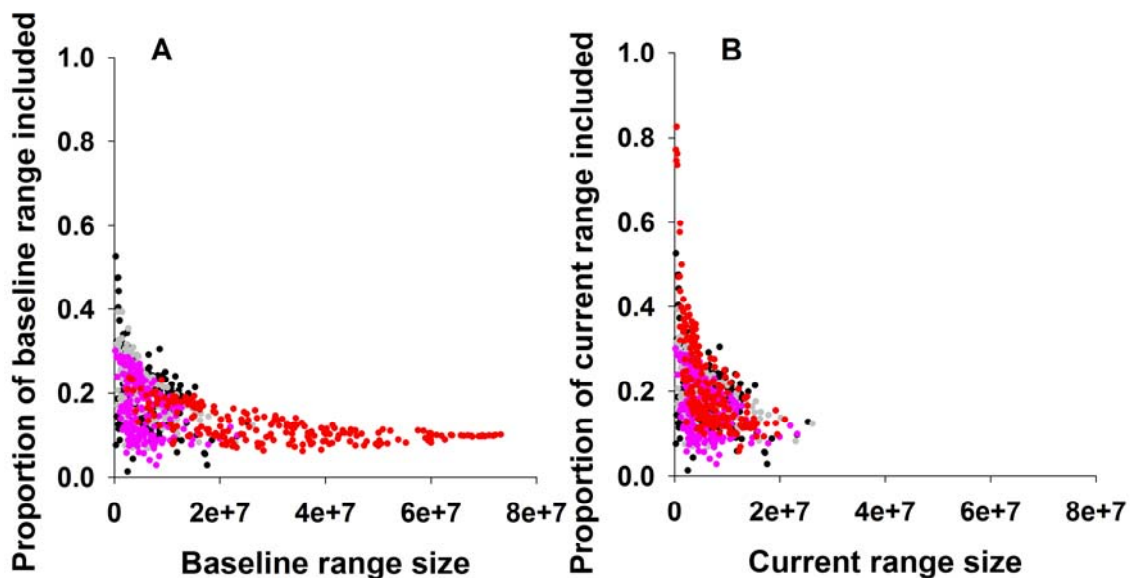


**Figure S4. The cost for each taxonomic group of protecting all other species.** For each taxon, the potential risk (*S17*) is shown for the taxon under its own single-taxon solution (Ants = red, Butterflies = blue, Frogs = cyan, Geckos = pink, Lemurs = brown, Plants = green) and under the multi-taxon solution (hatched). Note that the potential extinction risk is based both on forest losses incurred since 1950 and losses expected in the future under the not unwarranted assumptions that all forests outside of reserves will be lost (*S34*), and that the majority (estimated at 90%, *S35*) of Malagasy species are forest-dependent. The group with the highest cost (mantellid frogs) is estimated to increase in extinction risk by a factor of 1.6; in contrast, plants (which constitute the largest species group) experience essentially no change among the two scenarios.

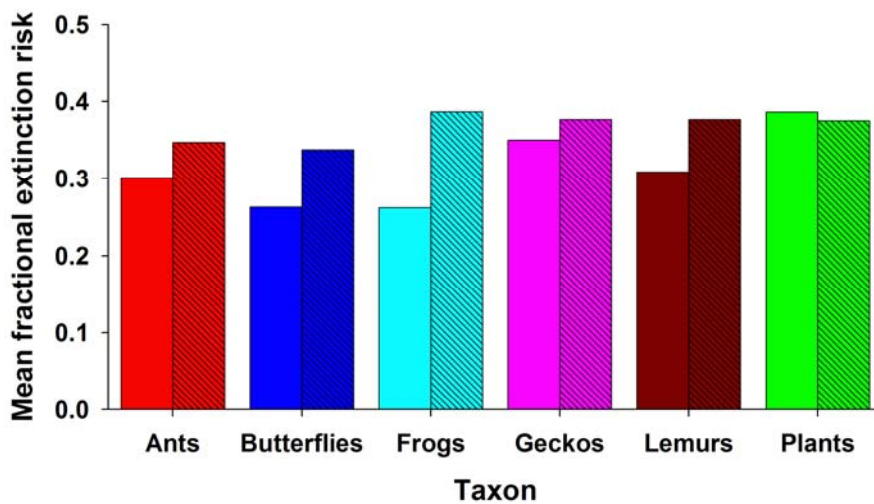


**Figure S5. Gap analysis for the actual and optimized unconstrained protected areas.** The percent species represented in the actual protected area network (red = 829 modeled species, blue = 1486 RTS; black = all species) at each phase of network expansion (October 2002 = 2.9%, December 2005 = 4.5%, June 2006 = 4.7%, December 2006 = 6.3%). White dots show the percent representation for all species together under the optimized, unconstrained solution (shown in Fig. 2a) at equivalent landscape areas; results are similar for the constrained solution. At the current rate of increase, not all species will be represented at the target of 10% of Madagascar's land surface protected, unless optimization methods are adopted.

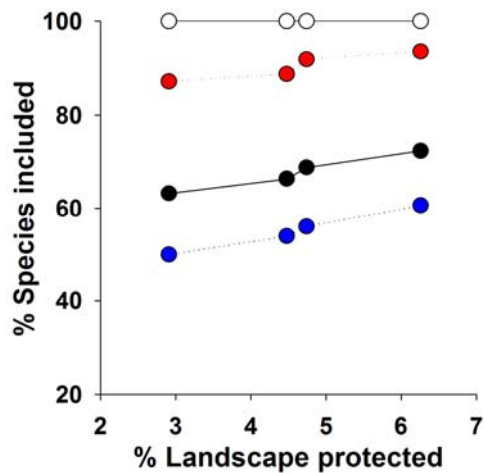


### Figure S6. Proportional representation at sequential stages of park expansion.

For included (non-GAP) species only, the mean and standard error of the percent of actual occurrences included per species is shown for RTS (blue) and modeled species (red) at each phase of network expansion (October 2002 = 2.9%, December 2005 = 4.5%, June 2006 = 4.7%, December 2006 = 6.3%). All RTS can be included at a mean proportional representation of  $99.9\% \pm 0.1\%SE$  of occurrences in the optimized constrained solution.

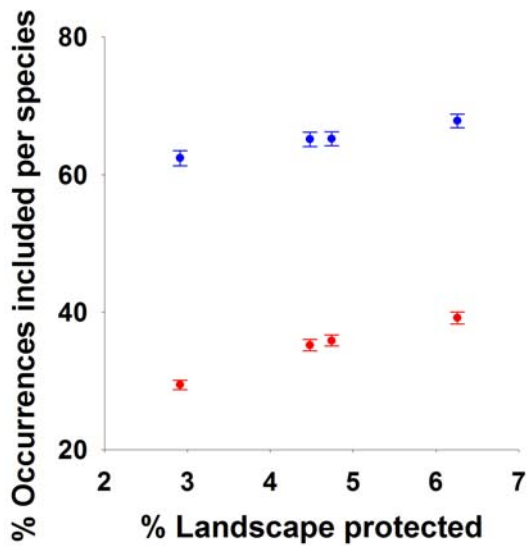
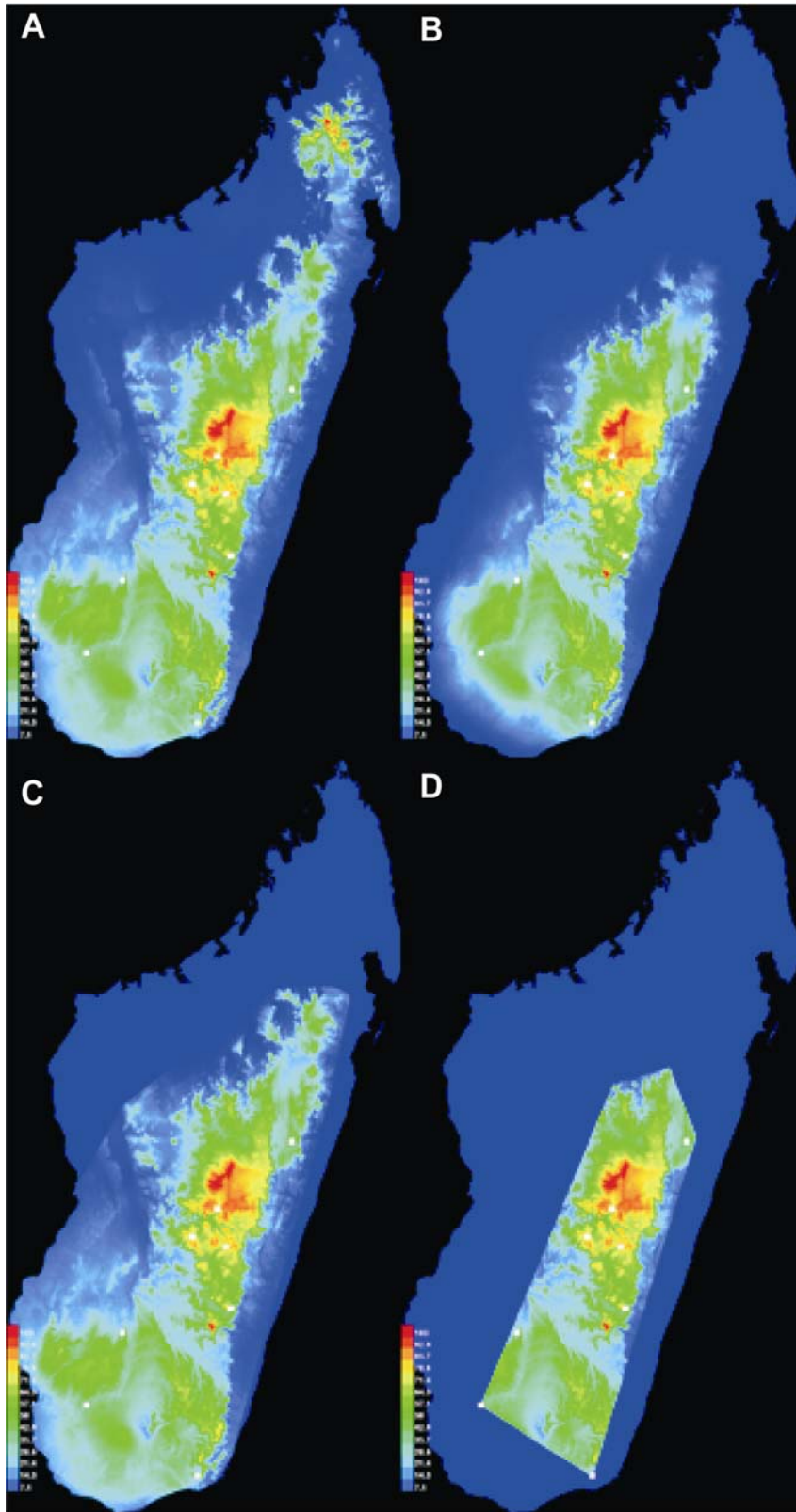


**Figure S7. Full hierarchical ranking of the constrained multi-taxon solution.**

The full hierarchical ranking of the Zonation solution, from lowest priority to highest priority of the landscape. The lowest ranked 27% of Madagascar is indicated in grey with no intermediary rankings. In order to conduct the Zonation run at this resolution and with this many taxa, the number of grid cells considered had to be reduced, as described in the text above and as illustrated in Figure S11. Thus, from the 27% removal rank (73% of landscape remaining) up to the 100% (0% of landscape remaining), the priority ranking ranges from pale pink (lowest conservation priority) through red to black (highest priority). The top 10% of the landscape (90-100%) corresponds to the proposed solution shown in Figure 2b, which also shows internal rankings within the top 10% in three categories.



**Figure S8. The effect of correcting for over-prediction.**



For the butterfly *Actizera atrigemmata* the map shows habitat suitability from high (red) to low (blue), with white dots indicating actual observations of the species (11 independent records, not all are visible due to the size of the image). a. uncorrected. b. Biogeographic correction, version 1. c. Biogeographic correction, version 2. d. Biogeographic correction, version 3. Parameter settings for biogeographic corrections for versions 1-3 are listed in the text.



**Figure S9. Full hierarchical ranking of landscape priority by Zonation.**

a. Full hierarchical output from Zonation for the ants' single taxon solution. Pale pink indicates the lowest 10% of the landscape, black indicates the highest 10%. Fig S1a (see supplementary results) shows only the top ten percent of this solution. b. Minimum (dashed), mean (solid), and maximum (dashed) proportions of ant species distributions included in the solution as landscape removal progresses. Corresponding mean potential extinction risk for the entire taxon (red).

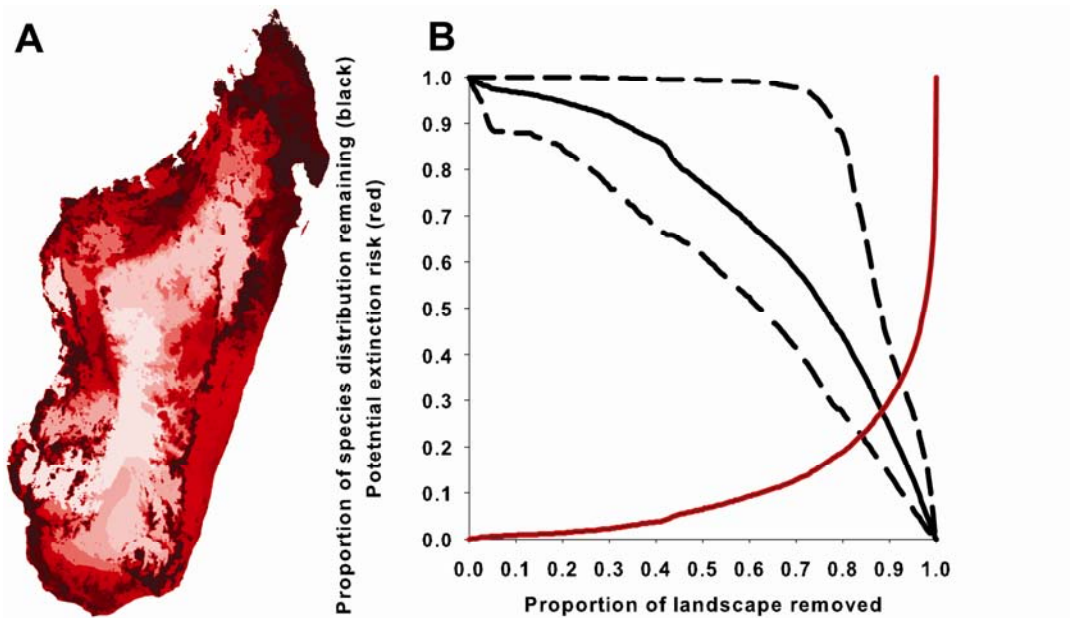


**Figure S10. Smoothing comparison.**

Unconstrained Zonation solutions (top 10%-ranked priorities) for all taxa combined including RTS species, a. without and b. with the smoothing parameter.

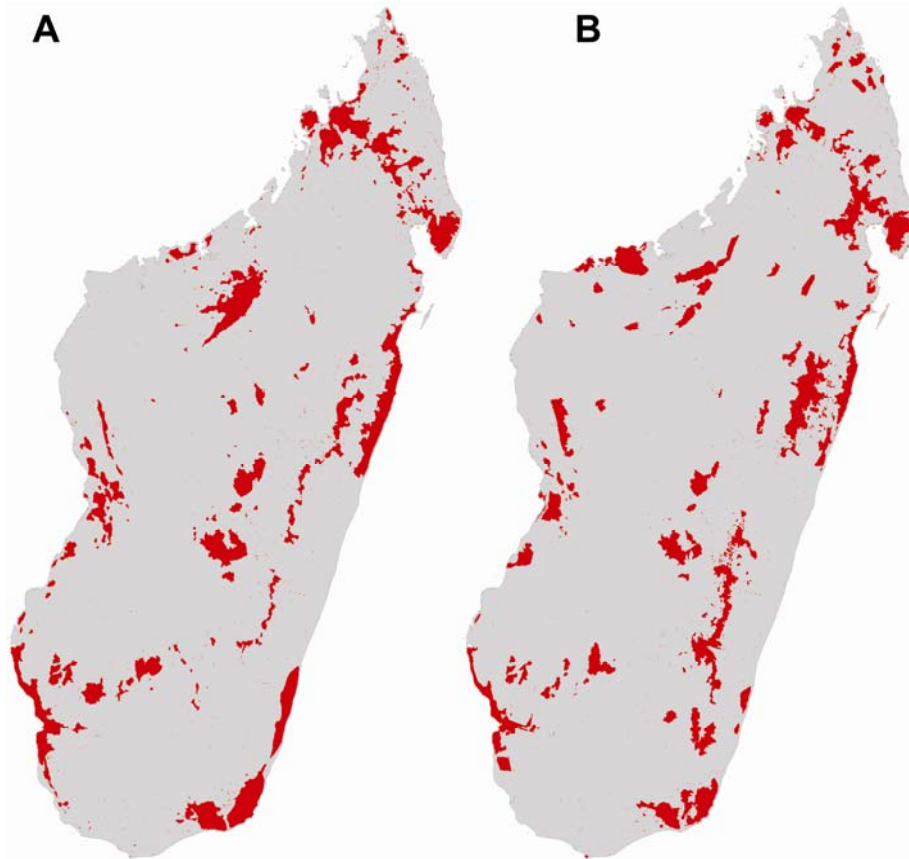


**Figure S11. The area of the country excised prior to the multi-taxon run.**

The cream-colored area was never selected in the top 25% of any taxon's Zonation solution for any of four run types (with and without smoothing, with and without RTS species). This region consists largely of heavily human-dominated, agricultural areas. The cream-colored area (27%), therefore, is the region that was excised from species models prior to conducting the all-taxon Zonation run; red indicates the region retained for conservation planning; black indicates the existing protected areas.

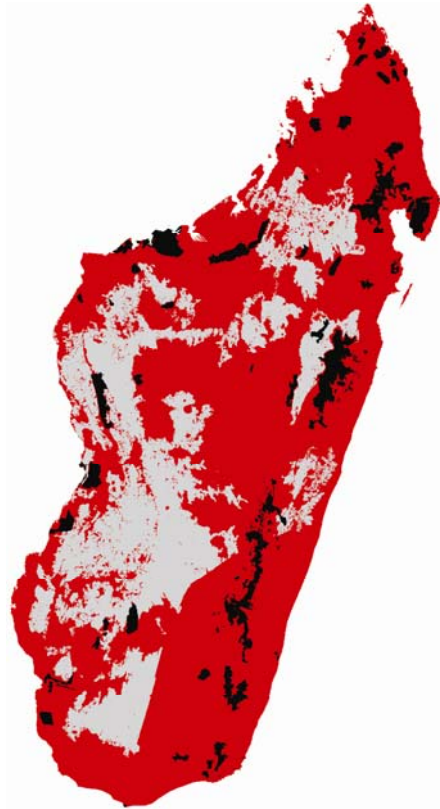


**Table S1. Taxonomic data utilized in distribution modeling and conservation planning.**

Endemism at the level of the entire taxon within the Malagasy sub-region (*S1, S37*) is noted based on (*S1*). Amassing this data involved data contributions from 21 scientists from 16 institutions spread through 6 countries.

Taxon	End-emism (%)	Modeled species	Unmodeled species	Data Providers	Source
Ants (leaf litter specialists, Family Formicidae <sup>1</sup> )	96%	73	253	BF	www.antweb.org
Butterflies	70%	171	131	DCL, CK, AC	( <i>S37- S42</i> )
Frogs (Family Mantellidae)	100%	20	179	DRV, MV, FG	( <i>S43</i> )
Geckos: genera <i>Phelsuma</i> and <i>Uroplatus</i> within Gekkonidae	83%	22	26	CR, RAN	( <i>S3</i> )
Lemurs	100%	31	14	EL, PCW	( <i>S44- S51</i> )
Plants (Family Arecaceae, Tribe Coleeae, plus the APAPC <sup>2</sup> dataset)	83%	512	884	GS, APAPC dataset; MZ, TG, Coleeae; JD, HB, Arecaceae	( <i>S19- S23, S52, S53</i> )
<b>TOTALS</b>		<b>829</b>	<b>1486</b>		

1. Primarily in the tribe Dacetini and the sub-families Amblyoponinae, Ponerinae, and Cerapahcyinae

2. The APAPC dataset (Missouri Botanical Garden's Assessment of Priority Areas for Plant Conservation) includes all point occurrence data for 1175 endemic species, representing the variety of families, eco-regions and plant life forms that occur in Madagascar.